Water Air Soil Pollut (2020) 231: 215
https://doi.org/10.1007/s11270-020-04586-y

# Removal of Estradiol from Water with a Hybrid MIP-$TiO_2$ Catalytic Adsorbent

**Marina Caldeira Tonucci · Leandro Pablo dos Santos Xavier · Adilson Candido da Silva · Sergio F. Aquino · Bruno Eduardo Lobo Baeta**

Received: 8 December 2019 / Accepted: 8 April 2020 / Published online: 3 May 2020


**Abstract** 17β-Estradiol (E2) is one of the main compounds responsible for estrogenic activities in sewage and natural waters and has been found in these matrices all around the world, thereby justifying the development of technologies for its removal. In this work, pure or $TiO_2$-containing molecularly imprinted polymers (MIPs) and non-imprinted polymers (NIPs) were prepared using E2 as template. The materials were characterized by infrared spectroscopy, X-ray diffraction, adsorption/desorption of $N_2$, and scanning electron microscopy (SEM). The characterization analyses showed that $TiO_2$ was incorporated in the polymers and that all materials could be characterized as mesoporous and had surface areas ranging from 238 to 279 $m^2g^{-1}$. Adsorption studies showed MIP-$TiO_2$ had a high capacity to adsorb E2 from the water phase leading to $q_{max}$ values of 15.16 to 26.49 mg $g^{-1}$ at temperatures from 25 to 45 °C, respectively. In addition, the thermodynamic study showed that the adsorption process is endothermic, spontaneous, and entropically driven. The results also showed that the presence of $TiO_2$ decreases the adsorption performance of MIP-$TiO_2$ when compared with MIP (without the photocatalyst) during the adsorption. However, the application of MIP-$TiO_2$ in a process of adsorption followed by photocatalysis resulted in 100% of E2 removal allowing the reuse of adsorbent. In addition, MIP-$TiO_2$ maintained its E2 removal capacity even after five cycles of regeneration–reuse, which shows the ability of UV light to regenerate the specific adsorption sites. The results presented in this paper show MIP-$TiO_2$ has potential to be applied in water treatment systems to remove E2.

**Keywords** 17β-Estradiol · Titanium dioxide ($TiO_2$) · Molecularly imprinted polymer (MIP) · Photocatalysis · Adsorption

M. C. Tonucci · L. P. dos Santos Xavier · A. C. da Silva · S. F. Aquino · B. E. L. Baeta (✉)
Laboratory of Technological and Environmental Chemistry, Department of Chemistry, Institute of Exact and Biological Sciences (ICEB), Campus Morro do Cruzeiro, Federal University of Ouro Preto (UFOP), Ouro Preto, Minas Gerais 35400-000, Brazil
e-mail: brunobaeta@ufop.edu.br

## 1 Introduction

The presence of endocrine-disrupting chemicals (EDCs) in water has become a great concern to society due to their ability to adversely affect aquatic life and pose a risk to human health. These compounds are natural or synthetic chemicals capable of interfering in the normal functioning of the hormonal system by mimicking or antagonizing the effects of hormones, by altering the pattern of synthesis and metabolism of hormones, and by modifying hormone receptor levels (Kümmerer 2009).

17β-Estradiol (E2) has been identified as one of the main compounds responsible for estrogenic activities in wastewater treatment plants (WWTP) (Lee et al. 2005). It is used as the main active principle in contraceptive drugs or medication for menopause and hormone replacement therapy. After being used, it might be

excreted in its original form or as metabolites to reach the aquatic environment via sewage discharge. Conventional water treatment plants (WTPs) adopt clarification processes (coagulation, flocculation, sedimentation, and filtration) followed by disinfection which have little effect on the removal of estrogenic compounds, such as E2 (Xavier et al. 2019).

In view of these concerns, different technologies have been studied to effectively remove EDCs from water. Adsorption with activated carbon (powdered (PAC) or granular (GAC)) is the most applied technique to remove dissolved compounds from water. However, besides not degrading the contaminant, the low selectivity of PAC or GAC can preclude their use to remove specific estrogenic compounds from water (Li et al. 2006; Saavedra et al. 2017, 2018). An efficient alternative way for removing EDCs from water and wastewater is the so-called advanced oxidation processes (AOP). An example of AOP is the heterogeneous photocatalysis, which employs a semiconductor, such as titanium dioxide ($TiO_2$), capable of generating hydroxyl radicals (*OH) responsible for the oxidation of several organic microcontaminants (Oliveira et al. 2015; Oi et al. 2016). However, since hydroxyl radicals are not specific and oxidize different reduced compounds, photocatalysis might become an expensive treatment process, thereby hindering its direct use in complex matrices such as sewage and contaminated waters. Moreover, the addition of heterogeneous photocatalyst in the water medium increases operational costs if the material is not recovered to be further reused (Li Puma et al. 2010; Paz 2010).

A promising alternative to avert these problems is to synthesize a molecularly imprinted polymer (MIP) containing the photocatalyst $TiO_2$ (Xu et al. 2014; Lai et al. 2016). MIPs are materials that can be synthesized to specifically adsorb a target molecule (Zhao et al. 2015; Barros et al. 2016) since they have selective cavities, which mimics a key-lock interaction. Thereby, molecularly imprinted polymer containing $TiO_2$ creates a highly favorable material for the combination of adsorption and photodegradation processes. MIP-$TiO_2$ might favor the mass transfer of the target molecule from the aqueous phase to its surface which contains the catalyst which upon receiving UV light is responsible for generating the oxidizing species that degrades the pollutant and regenerates the adsorption sites. Therefore, the aim of this study was to synthesize MIP containing $TiO_2$ particles to evaluate its efficiency in the removal of E2 from aqueous samples.

## 2 Materials and Methods

### 2.1 Synthesis of Molecularly Imprinted Polymers

The reagents applied in the MIP synthesis were E2 as the template, methacrylic acid (MAA) as the functional monomer, trimethylolpropane trimethacrylate (TRIM) as the cross-link agent, 2,20-azoisobutyronitrile (AIBN) as the radical initiator, and chloroform:dimethyl sulfoxide (1:1 v/v) as a porogenic solvent mixture. All reagents used in this study were obtained from Sigma-Aldrich.

The synthesis of MIPs coupled with $TiO_2$ and its respective blank polymers (NIP) was performed through a similar bulk polymerization. The template was dissolved in 8.0 mL of solvent under intermittent mixing. After 30 min, the cross-link agent, the radical initiator, and 100 mg of the photocatalyst ($TiO_2$) were added. Following a brief homogenization, the flask was purged with $N_2$ in order to remove oxygen, and then it was sealed and heated to 60 °C for 24 h. After $TiO_2$ synthesis, only approximately 30% of the added $TiO_2$ mass was incorporated into the polymeric matrix. The template extraction from the MIPs was carried out with methanol and acetic acid (9:1 v/v) in a Soxhlet system as described by Shen et al. (2012).

### 2.2 Material Characterization

FTIR analysis was used to identify the main functional groups present on the surface of MIP-$TiO_2$ and NIP-$TiO_2$. The analyses were carried out in ABB Bomem MB 3000 spectroscopy equipment with a resolution of 4 $cm^{-1}$, 32 scans per sample, from 400 to 4000 $cm^{-1}$. Samples were mixed with KBr (spectroscopic grade) at a 0.3% ratio and then homogenized and pressed to obtain a uniform pellet.

The specific area of the synthesized materials was estimated by determining the amount of nitrogen gas required to form a monolayer on the surface of the solid. The samples were degassed at 150 °C for 6 h and then analyzed in a Quantachrome NOVA 1200E equipment.

Scanning electronic microscopy (SEM) was employed to obtain the morphological properties of the

surface of MIP-$TiO_2$ and NIP-$TiO_2$, by using a JVM JSM 6010LA equipment.

### 2.3 Estradiol Analysis

Estradiol concentration was measured by a high performance liquid chromatograph (HPLC), model 20A (Shimadzu®, Tokyo, Japan) fitted with a Restek C18 column duly kept at 50 °C. The mobile phase was water:acetonitrile (6:4 v/v) at the flow rate of 0.20 mL $min^{-1}$. Estradiol detection was with a UV-Vis detector at the wavelengths of 198 and 280 nm. The chromatographic sample was prepared by adding an aliquot of 600 μL of the aqueous sample (previously centrifuged at 5000 rpm for 5 min) in a 1.5-mL vial containing 400 μL of acetonitrile.

When estradiol was present in low concentrations, such as at the end of the adsorption/photodegradation studies, its quantification was also determined by gas chromatography coupled to mass spectrometry (GC-MS). The GC-MS (model QP2010S-Plus, Shimadzu®) used was equipped with automatic sampler (model AOC-20i, Shimadzu®) and electronic flow control. The aqueous samples were centrifuged and freeze-dried (1.0 mL) and then submitted to a derivatization step using N,O-bis(trimethylsilyl)trifluoroacetamide (BSTFA).

### 2.4 Adsorption Isotherms and Kinetic Studies

Estradiol adsorption isotherms were obtained according to the following procedure: 20.0 mL of estradiol solutions with concentrations between 0.1 and 2.4 mg $L^{-1}$ was added to 10 amber flasks of 35 mL and kept under stirring (160 rpm) in a shaker incubator for 30 min at different temperatures (15 ± 0.5 °C, 25 ± 0.5 °C, 35 ± 0.5 °C, and 45 ± 0.5 °C) to obtain the thermodynamic parameters. Once the temperature had stabilized, 1.0 mg of adsorbent was added to each flask, followed by incubation and stirring for 3 h at 160 rpm. After the incubation period, an aliquot of 2 mL of each solution was centrifuged at 5000 rpm for 5 min so that the supernatant could be analyzed for estradiol in the HPLC or GC-MS systems.

The kinetic assays were performed in 11 amber flasks of 35 mL containing 20 mL of estradiol solution (1.4 mg $L^{-1}$) and 1.0 mg of adsorbent. The flasks were incubated under intermittent stirring at 160 rpm and 25 °C. Aliquots of the solutions were sampled at fixed times (0, 1, 5, 10, 15, 30, 45, 60, 75, 90, and 120 min) and centrifuged before analysis in the HPLC system. The conditions for the adsorption and kinetic assay such as amount of adsorbent were previously optimized by Xavier et al. (2019).

### 2.5 Photodegradation Studies

#### *2.5.1 Simultaneous Estradiol Adsorption and Photodegradation: Single Stage*

The aim of this assay was to evaluate the efficiency of MIP-$TiO_2$ in the removal of estradiol from aqueous samples. For this, 50 mg of adsorbent (MIP-$TiO_2$) was added in 400 mL of E2 solution (2.0 mg $L^{-1}$) and kept under stirring at 160 rpm for 4 h. The mass of adsorbent was calculated considering the amount of estradiol present in the reactor and the $q_{max}$ (mg $g^{-1}$) of 15.16 (Table 2) obtained during the isotherm study, considering a desirability removal of 100% of estradiol. In the first 60 min, the lamp was off and, after this time, the lamp was switched on until the end of the assay. Simultaneously, another procedure was performed, differing only by the fact the lamp was kept off throughout the assay. Samples were collected at 0, 15, 30, 45, 60, 90, 120, 150, 180, 210, and 240 min for HPLC analysis; and those samples collected at 60 min onwards were also analyzed by GC-MS. In addition, the samples collected at 0, 60, 150, and 240 min were submitted for TOC analysis.

#### *2.5.2 Estradiol Adsorption Followed by Photodegradation: Double Stage*

The objective of this assay was to evaluate the efficiency of E2 removal by MIP-$TiO_2$ in a two-step process: The first one was for the selective adsorption of E2 from the water matrix, and the second one was for the photocatalytic regeneration of the adsorbent in another flask reactor. For this, 50 mg of adsorbent was added in a flask containing 400.0 mL of E2 solution (2.0 mg $L^{-1}$). After 2 h of stirring (160 rpm), the mixture was filtered, and an aliquot of the aqueous phase was analyzed by HPLC. The remaining solid was transferred to another flask containing 400.0 mL of distilled water, and the adsorbent (MIP-$TiO_2$) was submitted to photodegradation by irradiating the suspension with a UVC lamp. After this procedure, the mixture was filtered, and the solid obtained was dried at 50 °C for 24 h.

After drying, the adsorbent was reused for E2 removal. This cycle was performed 5 times to evaluate the efficiency of such a procedure in regenerating the MIP-$TiO_2$ adsorbent.

## 3 Results and Discussion

### 3.1 Material Characterization

According to the data presented in Table 1, it can be observed that $TiO_2$ has a low specific area, which makes its direct application as adsorbent with photocatalytic properties difficult, as the mass transfer of pollutants from the solution to the surface of the catalyst would be limited. Other authors such as Nawi and Zain (2012), Kalan et al. (2016), and Shayegan et al. (2018) also observed low values of the surface area for the $TiO_2$ P25. When comparing the materials synthesized with and without $TiO_2$, it is observed that the photocatalyst generates a small decrease in the surface area and volume of micropores, which may also contribute to reducing the adsorption capacity of the materials. In relation to the average pore diameter, a little decrease is noticed in the volume of micropores when $TiO_2$ is added to the polymer. Indeed, according to IUPAC classification, it is observed that the polymers are predominantly mesoporous. Larger pore sizes facilitate the diffusion through the solid of bigger and complex molecules such as the case of estradiol.

In order to evaluate if the MIP synthesis caused some changes to the photocatalyst which could impair its photocatalytic capacity, XRD analyses of the adsorbents and $TiO_2$ were carried out as presented in Fig. 1a. Likewise, FTIR analyses (Fig. 1b) of the synthesized materials were also carried out to see whether the addition of $TiO_2$ significantly changed the polymers' surface properties.

From Fig. 1b, the bands corresponding to the characteristic groups for these MIPs and NIPs are seen. The band at 1750 $cm^{-1}$ reflects the carbonyl group (C=O) of the carboxylic acid (MAA) used as a monomer evidencing the predominance of this group in the polymers, whereas the band at 1638 $cm^{-1}$ is due to C=C stretching which indicates the presence of the vinyl group. It is also observed that there was no significant difference in the band's profile after the introduction of $TiO_2$, except by subtle differences in the peak intensities, which can be attributed to the "dilution effect" due to the presence of $TiO_2$ in the polymeric matrix.

In Fig. 2, the SEM images of the synthesized polymers are presented. SEM analyses indicate that the presence of $TiO_2$ caused significant changes in the physical characteristics of the adsorbent's surface. However, it is still possible to see the presence of pores in the MIP-$TiO_2$ but in smaller amounts. This is not desired since it can lead to a decrease in the adsorption capacity of the adsorbents containing $TiO_2$ in relation to those without it.

### 3.2 Isotherms and Thermodynamics of Estradiol Adsorption

Isotherms were performed at temperatures of 15, 25, 35, and 45 °C, which allowed the thermodynamic evaluation of the process. Figure 3 presents the isotherms at different temperatures for each adsorbent, adjusted according to the multilayer adsorption model, which best fitted the experimental data. The main parameters of the nonlinear modeling of the isotherms are presented in Table 2.

As can be observed, the adsorption capacity of estradiol by the synthesized materials generally increases with temperature, suggesting that the process is endothermic. It is also observed that in all cases the MIPs were able to adsorb a higher amount of E2 than their respective NIPs, and that the incorporation of $TiO_2$ into the polymer caused a decrease in the adsorption capacity which might have been due to the changes in adsorption area and pore size, as previously discussed.

Although the multilayer model best fitted the data, its constant $k_a$ is equivalent to the Langmuir constant $b$, when $n$ assumes the value of 1. This allows one to estimate the value of the RL separation constant, as shown in Table 2. As the RL values were between 0 and 1, it is possible to state that the adsorption is favorable in all temperatures studied and its irreversibility increases as the temperature increases.

In order to determine the thermodynamic parameters of the adsorption process, the data of Fig. 3 were processed as shown in Table 3. Lee and Doong (2012) studied the adsorption of estradiol and also found positive values for the adsorption enthalpy (84.50 kJ $mol^{-1}$), which was of the same magnitude of the values found in this work, confirming that the retention of estradiol on the surface of adsorbents is of an endothermic nature. A hypothesis to explain these

**Table 1** Surface area obtained by BET analysis of $N_2$ adsorption data for MIPs and NIPs

| Material | Specific area ($m^2$ $g^{-1}$) | Micropore volume ($cm^3$ $g^{-1}$) | Average pore diameter (*A*) |
|---|---|---|---|
| MIP | 254 | 0.137 | 15.919 |
| NIP | 279 | 0.146 | 16.383 |
| MIP-$TiO_2$ | 238 | 0.134 | 18.572 |
| NIP-$TiO_2$ | 245 | 0.126 | 19.297 |
| $TiO_2$ | 9 | 0.005 | 66.327 |

observations relates to the solvation of the estradiol molecule in the presence of methanol (added in a ratio of 1:5000 to prepare the solution), as represented in Fig. 4. It was also observed that the addition of $TiO_2$ to the polymer caused an increase in the value of the thermodynamic parameters, as observed by Zhang et al. (2013). This indicates that the adsorption of E2 onto MIP-$TiO_2$ should be a little more difficult, which, together with other factors, may explain the fact that this adsorbent had a lower adsorption capacity of such estrogen when compared with the polymers without $TiO_2$.

According to Table 3, it is observed that the Gibbs free energy variation ($\Delta G°$) became more negative as the temperature increased, indicating that the process is more spontaneous at higher temperatures ($\Delta G° = \Delta H° - T\Delta S° < 0$). The positive enthalpy values found for estradiol adsorption indicate that the process is endothermic. As the entropies found were also positive, to satisfy the equality, it is necessary that $T\Delta S° > \Delta H°$. Therefore, the increase in the degrees of freedom at the adsorbent interface is the determining factor for the adsorption process. In other words, when the estradiol molecules are adsorbed, the system appears to be more disorganized, and this seems contradictory since the adsorption involves a greater organization of adsorbates on the surface of the adsorbent. However, as previously discussed, the solvation of estradiol molecules brought about by methanol addition increased the degree of freedom and might help explain this apparent contradiction. Knowing that the estradiol molecule is very hydrophobic, it can be inferred that methanol, even in small amounts, acts to form a complex with E2 during its dissolution. As exemplified in Fig. 4, methanol might interact with the polar part of E2 by Van der Waals forces, leaving its hydroxyl group free to interact with water or methanol by means of hydrogen bonds.

Thus, for estradiol adsorption onto MIP-$TiO_2$ to occur, the interactions between E2 and water or methanol are disrupted to form adsorbent-adsorbate interactions. This process demands energy, which may explain the fact that adsorption of E2 onto MIPs and NIPs was endothermic. In addition, the molecules appear to be more organized when forming the aqueous complex, so that after breaking the intermolecular interactions, there is an increase in the degrees of freedom of the

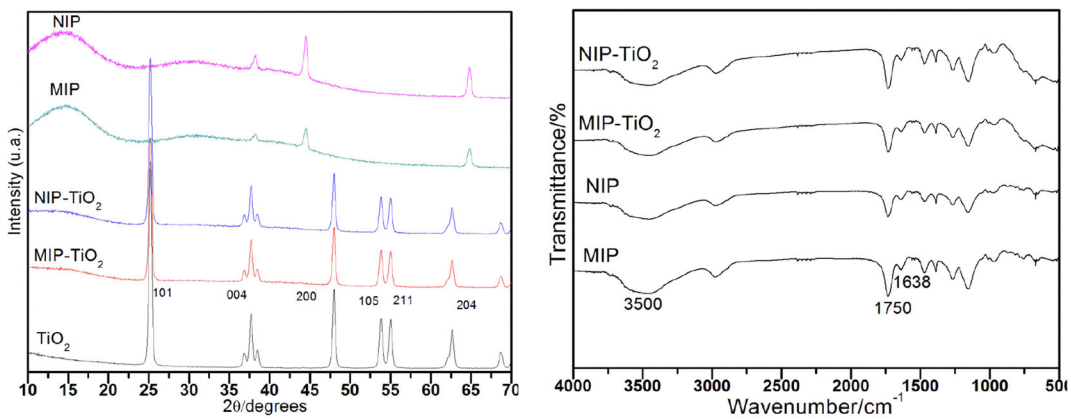


**Fig. 1** **a** XRD diffractograms and **b** infrared spectra for MIPs and NIPs without and with $TiO_2$

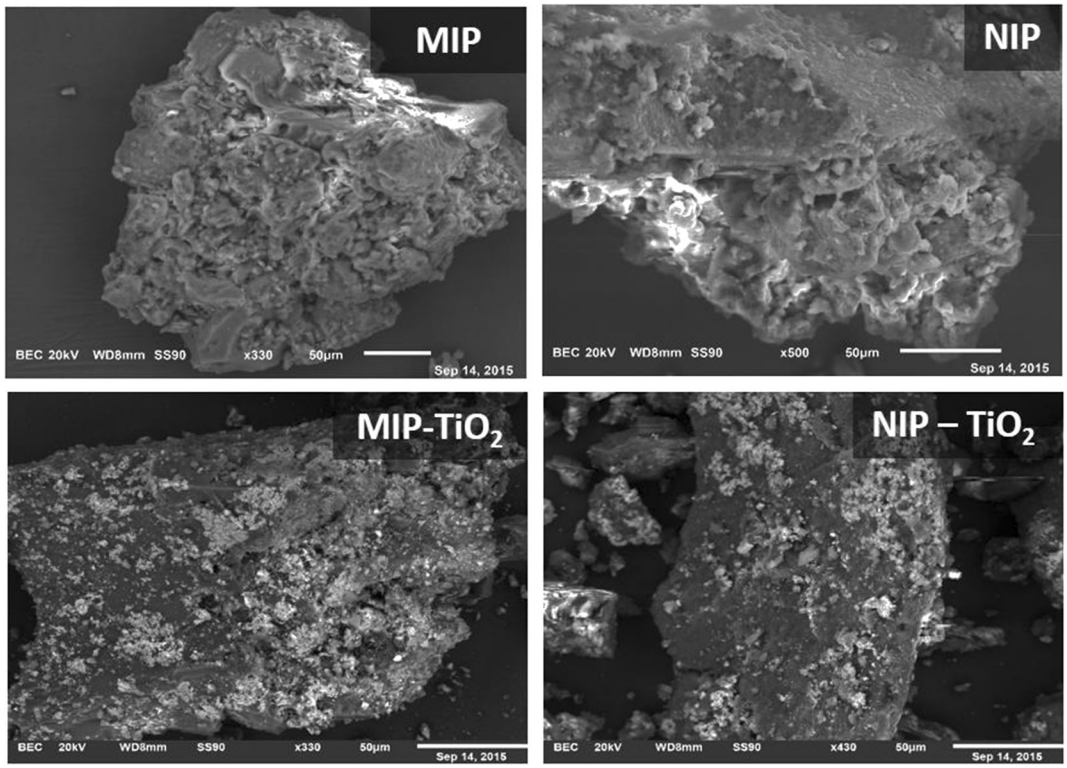


**Fig. 2** Scanning electron microscopy images of MIPs and NIPs without or with $TiO_2$

system, which justifies the negative values of free energy change ($\Delta G < 0$).

The adsorption process can be classified as chemical or physical according to the magnitude of the enthalpy. Values of enthalpy lower than 84 kJ $mol^{-1}$ are typical of physical adsorption, since the energies of chemical bonds vary from 84 to 420 kJ $mol^{-1}$. Thus, it is hypothesized that the adsorption of estradiol onto MIPs occurred by means of chemical bonds, which are highly energetic and specific. On the other hand, when the NIPs are considered, the adsorption process seems to have a physical character, probably by means of the low-intensity forces of Van der Waals, as is to be expected for hydrophobic molecules such as estradiol.

### 3.3 Kinetics of Estradiol Adsorption

The data obtained in the kinetic assays were modeled by the pseudo-second order (Fig. 5 and Table 4) and intraparticle diffusion (Table 5) models. From Fig. 5, it can be observed that the data corroborate those presented in Table 2, at 25 °C (298 K), since the MIP exhibited higher adsorption capacity than the other materials. As described before, this might be due to the presence of $TiO_2$ which occupy some of the selective adsorption sites, besides hindering the diffusion of the adsorbate into the inner parts of the adsorbent. As expected, the NIPs exhibited lower adsorption capacities because they do not have specific adsorption sites.

From these data, it is observed that the higher the kinetic constant ($k^2$), the lower the adsorption capacity ($q_e$), which leads to the point already raised that, in a fast adsorption process, the molecules do not have time to organize themselves adequately on the surface of the adsorbent, or diffuse therefrom, resulting in lower adsorption capacity, which was confirmed by the intraparticle diffusion model.

It is also observed that the MIPs exhibited lower adsorption constant than the NIPs, thereby indicating that when using the latter, the adsorption process is very fast. This agrees with the results observed in the thermodynamic study, which shows that the energy involved in the adsorption of estradiol onto NIPs is smaller than in MIPs, being the process facilitated because it involves a physical adsorption. For MIPs, the energy demanded is higher because it involves the formation of

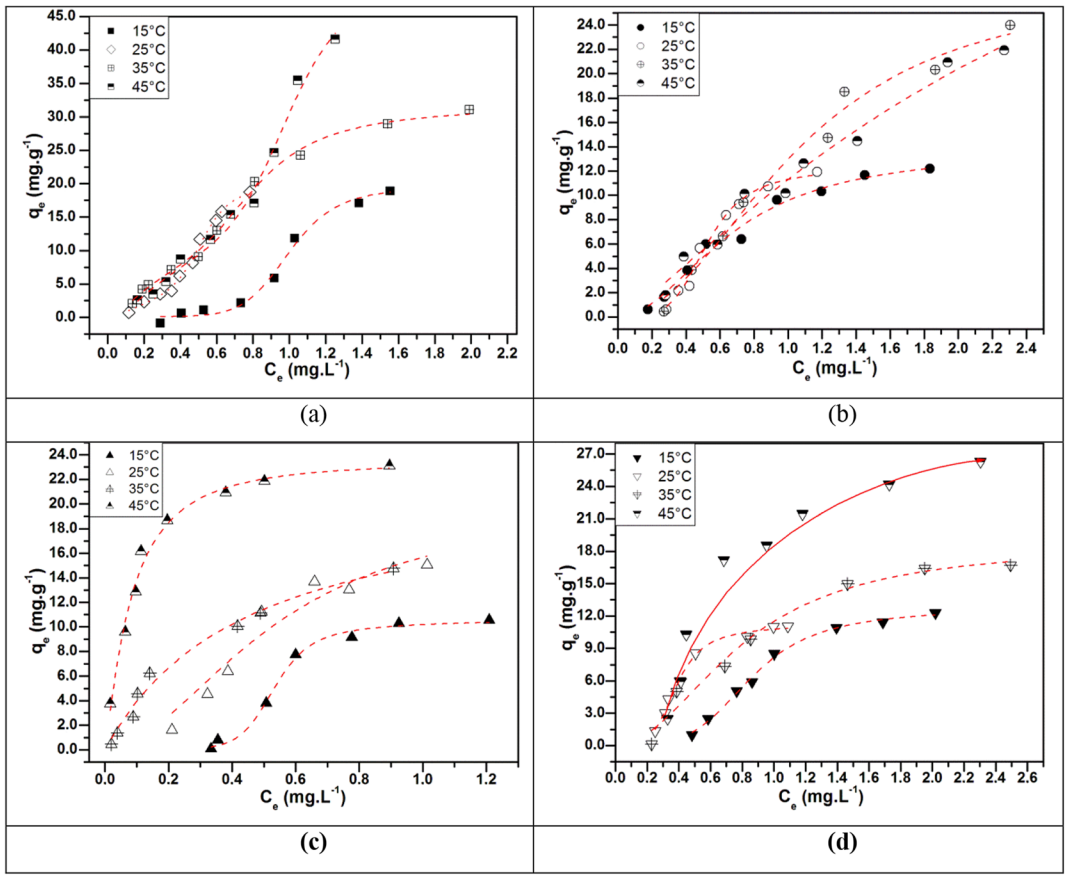


**Fig. 3** E2 adsorption isotherms. **a** MIP. **b** NIP. **c** MIP-$TiO_2$. **d** NIP-$TiO_2$

**Table 2** Isothermal parameters obtained for each adsorbent by adjusting the multilayer adsorption model to the experimental data

| Material/temperature | | | | | |
|---|---|---|---|---|---|
| | $T$ (°C) | 15 | 25 | 35 | 45 |
| | $T$ (K) | 288 | 298 | 308 | 318 |
| MIP | $q_{max}$ (mg g$^{-1}$) | 19.03 | 23.79 | 32.41 | 52.59 |
| | $k_a$ (L mg$^{-1}$) | 0.1236 | 0.3263 | 1.2360 | 5.8396 |
| | $r^2$ | 0.9885 | 0.9885 | 0.9996 | 0.9442 |
| | RL | 0.1468 | 0.0682 | 0.0073 | 0.0010 |
| NIP | $q_{max}$ (mg g$^{-1}$) | 13.80 | 12.13 | 27.57 | 26.49 |
| | $k_a$ (L mg$^{-1}$) | 0.0172 | 0.0677 | 0.1007 | 0.3431 |
| | $r^2$ | 0.9683 | 0.9735 | 0.9808 | 0.9707 |
| | RL | 0.6329 | 0.4090 | 0.0956 | 0.0317 |
| MIP-$TiO_2$ | $q_{max}$ (mg g$^{-1}$) | 10.39 | 15.16 | 15.04 | 26.24 |
| | $k_a$ (L mg$^{-1}$) | 0.0888 | 0.4094 | 2.2729 | 4.2101 |
| | $r^2$ | 0.9912 | 0.9693 | 0.9826 | 0.9366 |
| | RL | 0.2950 | 0.0839 | 0.0174 | 0.0066 |
| NIP-$TiO_2$ | $q_{max}$ (mg g$^{-1}$) | 13.22 | 11.57 | 18.71 | 24.52 |
| | $k_a$ (L mg$^{-1}$) | 0.0466 | 0.1209 | 0.1616 | 0.3083 |
| | $r^2$ | 0.9922 | 0.9917 | 0.9409 | 0.8840 |
| | RL | 0.3817 | 0.2890 | 0.0914 | 0.0351 |

**Table 3** Thermodynamic parameters of estradiol adsorption onto MIP, NIP, MIP-$TiO_2$, and NIP-$TiO_2$

| T (*K*) | | 288 | 298 | 308 | 318 |
|---|---|---|---|---|---|
| MIP | $k_a$ (L mol$^{-1}$) | $3.37 \times 10^4$ | $8.89 \times 10^4$ | $3.37 \times 10^5$ | $1.59 \times 10^6$ |
| | ln ($k_a$) | 10.42 | 11.40 | 12.73 | 14.28 |
| | $\Delta G_{experimental}$ (kJ mol$^{-1}$) | − 24.96 | − 28.23 | − 32.59 | − 37.75 |
| | $\Delta G_{theoretical}$ (kJ mol$^{-1}$) | − 24.51 | − 28.76 | − 33.01 | − 37.26 |
| | | ΔH (kJ mol$^{-1}$) | | 97.85 | |
| | | ΔS (kJ mol$^{-1}$) | | 0.42 | |
| NIP | $k_a$ (L mol$^{-1}$) | 4690.42 | 18,442.99 | 27,415.25 | 93,462.44 |
| | ln ($k_a$) | 8.45 | 9.82 | 10.22 | 11.45 |
| | $\Delta G_{experimental}$ (kJ mol$^{-1}$) | − 20.24 | − 24.34 | − 26.17 | − 30.26 |
| | $\Delta G_{theoretical}$ (kJ mol$^{-1}$) | − 20.47 | − 23.66 | − 26.85 | − 30.04 |
| | | ΔH (kJ mol$^{-1}$) | | 71.40 | |
| | | ΔS (kJ mol$^{-1}$) | | 0.32 | |
| MIP-$TiO_2$ | $k_a$ (L mol$^{-1}$) | 24,173.90 | 111,518.64 | 619,091.60 | 1,146,744.56 |
| | ln ($k_a$) | 10.09 | 11.62 | 13.34 | 13.95 |
| | $\Delta G_{experimental}$ (kJ mol$^{-1}$) | − 24.17 | − 28.79 | − 34.15 | − 36.89 |
| | $\Delta G_{theoretical}$ (kJ mol$^{-1}$) | − 24.44 | − 28.81 | − 33.19 | − 37.56 |
| | | ΔH (kJ mol$^{-1}$) | | 101.60 | |
| | | ΔS (kJ mol$^{-1}$) | | 0.44 | |
| NIP-$TiO_2$ | $k_a$ (L mol$^{-1}$) | 12,684.83 | 32,917.36 | 44,008.76 | 83,972.65 |
| | ln ($k_a$) | 9.45 | 10.40 | 10.69 | 11.34 |
| | $\Delta G_{experimental}$ (kJ mol$^{-1}$) | − 22.62 | − 25.77 | − 27.38 | − 29.98 |
| | $\Delta G_{theoretical}$ (kJ mol$^{-1}$) | − 22.88 | − 25.26 | − 27.63 | − 30.01 |
| | | ΔH (kJ mol$^{-1}$) | | 45.51 | |
| | | ΔS (kJ mol$^{-1}$) | | 0.24 | |

chemical bonds, which directly reflects the slower kinetics of the process.

When the diffusion model was used (figure not shown), the straight lines obtained by the adjustment

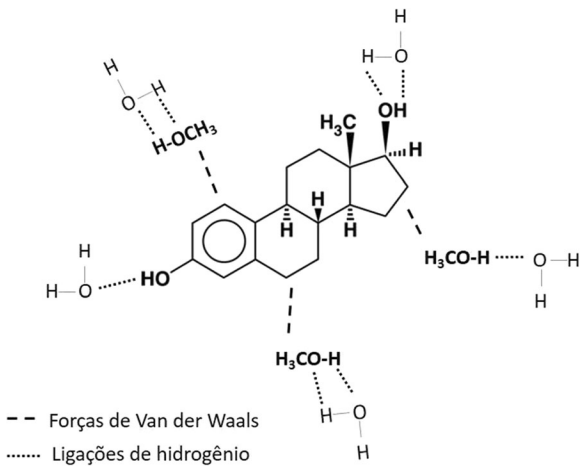


**Fig. 4** Schematic representation of the stabilization of E2 molecule in water by the presence of methanol

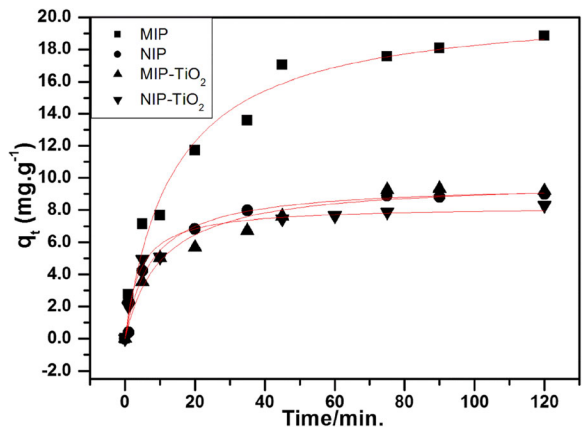


**Fig. 5** Fitting of the pseudo-second-order model to the experimental data of estradiol adsorption (2.0 mg L$^{-1}$, 25 °C) in MIPs and NIPs with and without $TiO_2$

**Table 4** Kinetic parameters of the pseudo-second-order model for the adsorption of estradiol (2.0 mg $L^{-1}$, 25 °C) in MIPs and NIPs with and without $TiO_2$

| Adsorbent material | $k^2$ | $q_e$ | $r^2$ |
|---|---|---|---|
| MIP | 0.00346 | 20.8 | 0.98 |
| NIP | 0.01370 | 9.6 | 0.99 |
| MIP-$TiO_2$ | 0.00974 | 9.9 | 0.96 |
| NIP-$TiO_2$ | 0.03000 | 8.2 | 0.98 |

did not intercept the axis at the origin (0, 0). In addition, it could be observed that the graphs exhibited multilinearity, thereby characterizing different stages of estradiol adsorption, which relates to its diffusion into the inner pores of the adsorbent. The first straight line obtained in the graph (step 1) represents the instantaneous estradiol adsorption on the external polymer surface, whereas the second straight line (step 2) is related to the gradual adsorption due to its intraparticle diffusion. By analyzing the slopes of the second step, it is observed that they were larger for the MIPs, indicating that for these materials, the diffusion interferes more by delaying the adsorption process when compared with NIPs. This corroborates what has been observed before when the pseudo-second model was fitted to the data, as well as the thermodynamic findings, thereby confirming the hypothesis that estradiol adsorption onto MIP might involve the formation of chemical bonds.

**Table 5** Kinetic parameters of the adjustment of the intraparticle diffusion model to the adsorption data of estradiol by MIPs and NIPs with and without $TiO_2$

| Adsorbent/parameter | | kD.I. (mg $g^{-1}min^{-½}$) | $q_e$ (mg $g^{-1}$) | $r^2$ |
|---|---|---|---|---|
| MIP | First step | 2.36 | 0.75 | 0.98 |
| | Second step | 0.59 | 12.43 | 0.99 |
| NIP | First step | 3.23 | 0.66 | 0.96 |
| | Second step | 0.31 | 6.42 | 0.94 |
| MIP-$TiO_2$ | First step | 1.28 | 0.51 | 0.94 |
| | Second step | 0.65 | 3.02 | 0.96 |
| NIP-$TiO_2$ | First step | 0.24 | 1.99 | 0.94 |
| | Second step | 0.42 | 5.03 | 0.97 |

### 3.4 Selectivity Experiment

The selectivity study was devised to evaluate if the materials produced in this work would keep the high capacities of molecular recognition even in the presence of competing molecules. Figure 6b shows the distribution coefficients obtained for adsorption of the microcontaminants E2, BPA, DCF, EE2, and E3 (whose structures are presented in Fig. 6a), when present in a multicomponent mixture, by the adsorbents synthesized in this study.

It can be seen in Fig. 6b that, for estradiol (E2), the values of the distribution constants $k_d$ were significantly higher for the MIPs than for the NIPs, which is a good indication of the molecular recognition of MIPs for estradiol, used as a template during its synthesis. The molecular recognition capacity of the MIP is even more evident when comparing the values obtained for E2 with those obtained for molecules with a similar structure, such as EE2 and E3. In the case of EE2, the ethyl group may cause a steric hindrance, making it impossible for the specific bonds to be efficiently formed. As for E3, in addition to presenting steric hindrance, it is more hydrophilic than E2, reducing its tendency to migrate from the liquid phase to the hydrophobic solid. In the NIPs, the adsorption of both EE2 and E3 was high, showing that the steric hindrance was not determinant since the adsorption is expected to occur superficially and in a nonspecific manner. In its turn, the contaminant DCF exhibited low $K_d$ values in all cases, and this is likely due to its high water solubility and low hydrophobicity. On the other hand, for BPA, a compound with a chemical structure very different from E2, its adsorption was probably due to physisorption due to its high hydrophobicity.

In order to better evaluate the efficiency of the imprinting process, the selectivity coefficients (kMIP and kNIP) were calculated and, from them, the relative selectivity coefficient, *k*', indicates the effectiveness of MIP (in relation to NIP) to adsorb estradiol instead of its competitors. These results are presented in Table 6. Values of *k*' greater than 1.0 indicate that the MIPs exhibited higher selectivity coefficients (*k*) for E2 in relation to the other contaminants than the NIPs. It is observed that E3 (with a structure similar to that of E2) had the highest *k*' values, indicating that the MIP was highly effective in differentiating the two molecules, despite their great similarities; this is further evidence the molecular imprinting process was efficient.

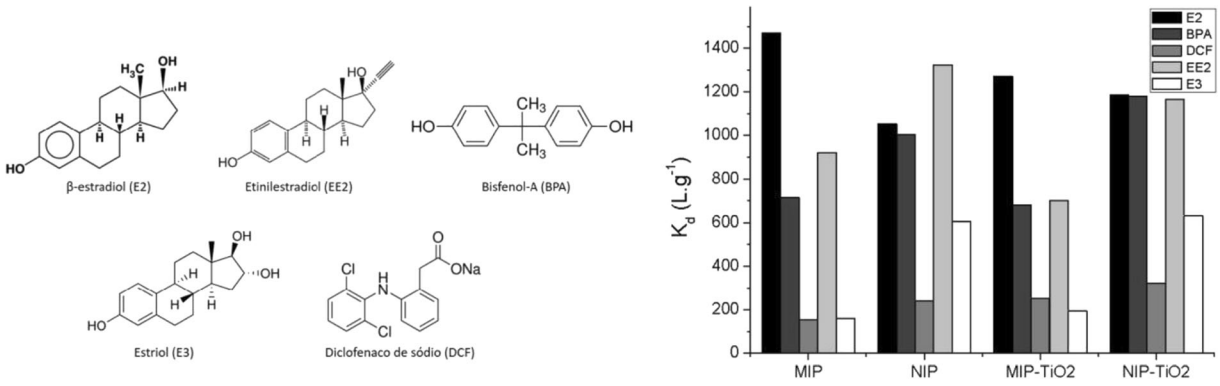


**Fig. 6** **a** Molecular structure of the microcontaminants used in the selectivity experiment. **b** Distribution coefficients ($k_d$) obtained for the adsorption of E2, BPA, DCF, EE2, and E3 onto the synthesized adsorbents

Comparing the polymers with and without $TiO_2$, it is observed that when adding the photocatalyst, a slight loss of selectivity occurs, as evidenced by the slight decrease in *k*' values. This was somehow expected since it has already been discussed the changes in the thermodynamic constants and morphological changes, such as surface area decrease, caused by the presence of the photocatalyst.

In spite of the slight decrease of the *k*' value when adding $TIO_2$, it is observed that for DCF there was an increase, implying that the presence of $TiO_2$ enabled a greater affinity of the MIP by this microcontaminant. A hypothesis that could explain this behavior is that the catalyst might cause changes in the surface charges of the polymer, which, depending on the test conditions (pH) and on the properties of the species involved (PCZ of adsorbent and pKa of the microcontaminant), can favor electrostatic attraction (diclofenac is a salt), thereby causing an increase of its adsorption onto the solid.

### 3.5 Estradiol Adsorption Associated with Its Photoregeneration

Figure 7 shows the results obtained in the tests where the adsorption and photodegradation processes were simultaneous, previously referred to as single stage. In all cases, the systems were kept under stirring for 60 min in the dark so that the adsorption equilibrium could be reached. After 60 min, the UV lamps were connected to

**Table 6** Selectivity parameters for estradiol adsorption onto MIPs and NIPs, with and without $TiO_2$, in the presence of competitive adsorbates

| Parameters/microcontaminant | | E2 | BPA | DCF | EE2 | E3 |
|---|---|---|---|---|---|---|
| MIP | $q_e$ (μg g$^{-1}$) | 110.0 | 28.1 | 12.7 | 51.4 | 12.2 |
| | $k_d$ (L g$^{-1}$) | 1471.2 | 714.3 | 153.5 | 920.8 | 159.7 |
| | kMIP | – | 2.1 | 9.6 | 1.6 | 9.2 |
| NIP | $q_e$ (μg g$^{-1}$) | 68.8 | 45.9 | 21.4 | 93.4 | 53.7 |
| | $k_d$ (L g$^{-1}$) | 1053.3 | 1005.2 | 239.8 | 1322.8 | 605.1 |
| | kNIP | – | 1.0 | 4.4 | 0.8 | 1.7 |
| MIP-$TiO_2$ | $q_e$ (μg g$^{-1}$) | 101.4 | 28.3 | 20.9 | 39.1 | 10.6 |
| | $k_d$ (L g$^{-1}$) | 1269.4 | 680.2 | 252.6 | 699.6 | 131.8 |
| | kMIP-$TiO_2$ | – | 1.9 | 5.0 | 1.8 | 9.6 |
| NIP-$TiO_2$ | $q_e$ (μg g$^{-1}$) | 81.1 | 77.1 | 27.7 | 85.9 | 54.1 |
| | $k_d$ (L g$^{-1}$) | 1187.1 | 1180.1 | 323.2 | 1166.6 | 631.0 |
| | kNIP-$TiO_2$ | – | 1.0 | 3.7 | 1.0 | 1.9 |

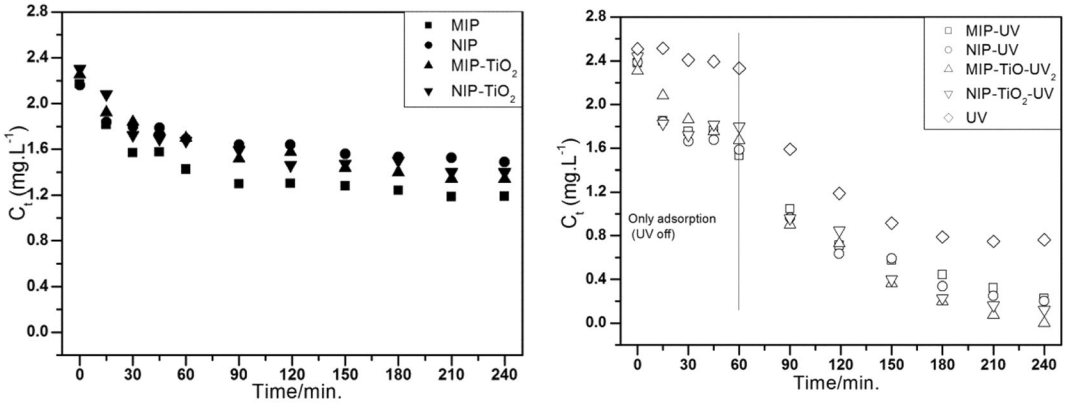


(a) (b)

**Fig. 7** Changes in estradiol concentration over time in the adsorption (**a**) and adsorption-photodegradation (**b**) assays

half of the flasks (Fig. 7b), including the control flask containing only the E2 solution (without the adsorbents). In the case of the non-irradiated tests, in which adsorption removal predominated (Fig. 7a), the difference between the final concentrations observed among the flasks containing different adsorbents was less than 0.4 mg $L^{-1}$ and resulted in a maximum estradiol removal of approximately 50% when MIP was used as adsorbent. When comparing the irradiated flasks with those without radiation, it was observed that when the UV lamp was switched on, there was a sudden drop in the estradiol concentration in the medium, even in the absence of adsorbent. This indicates that the radiation alone can provide moderate removal of E2 (about 70% when compared with the initial concentration) due to photolysis. This is because this estrogenic compound has high radiation absorption at 198 and 280 nm, which is very close to the emission wavelength (265 nm) of the UV-Vis lamps used in the experiment.

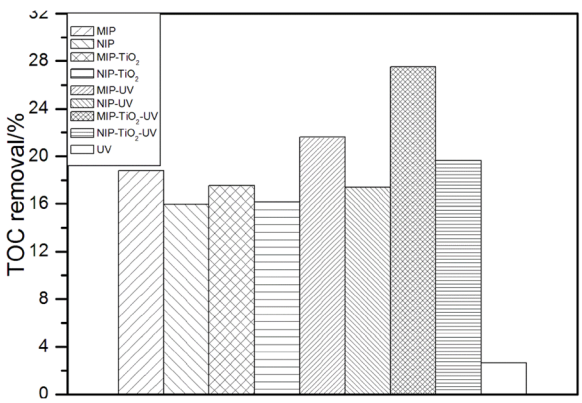


**Fig. 8** Removal of total organic carbon (TOC) in adsorption and adsorption-photodegradation assays

Figure 7b shows that when the process was only the adsorption, in the first 60 min of the process, the efficiency of the adsorption for the MIP was approximately 44%, while for the process when the UV light was turned on, it was ~ 41%, totaling an overall removal of 85%. For the MIP-$TiO_2$ material, the adsorption-only process was able to remove approximately 37%, while the adsorption process in conjunction with UV light was responsible for ~ 73% of the removal. When it evaluated only adsorption, MIP was more efficient; however, when was included the photocatalysis process together with adsorption, the MIP-$TiO_2$ material showed better efficiency, reaching a removal value 32% higher than that observed by MIP in the process involving adsorption and photocatalysis, showing the effect of immobilized $TiO_2$ in the MIP to improve estradiol removal. From the results, it is possible to verify that the

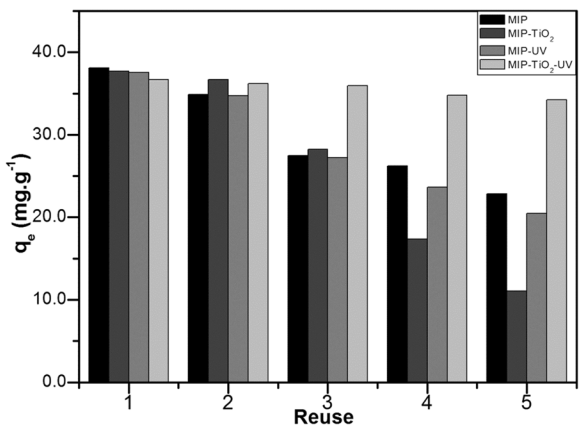


**Fig. 9** Changes in estradiol adsorption capacity ($q_e$, mg $g^{-1}$) by MIP and MIP-$TiO_2$ along the adsorption–regeneration cycles according to the double-stage process

photocatalysis in MIP without $TiO_2$ was responsible for 48% of the global removal and for MIP-$TiO_2$ the contribution was 73% of the global removal.

Figure 7b also shows that, in the presence of the adsorbents, estradiol removal was higher, reaching 100% for MIP-$TiO_2$, even though this hybrid material had lower adsorption capacity than MIP (see Fig. 7a). These results indicate that $TiO_2$ contributed positively to estradiol removal from water, probably because it enhances estrogen degradation, thereby freeing adsorption sites and allowing a higher removal of the contaminant from the medium.

Figure 8 shows the removal of TOC obtained at the end of the simultaneous adsorption and photodegradation tests. It is observed that in all cases, the use of UV light resulted in greater degradation of organic carbon than when the tests were run in the dark. In addition, estradiol degradation by photolysis (without the photocatalyst) led to a carbon removal of only 4%. On the other hand, when MIP-$TiO_2$ was used, it was observed that estradiol degradation was coupled to a higher degree of organic carbon removal. TOC removal increased from 18 (flasks with MIP and UV lamp on) to 28% (flasks with MIP-$TiO_2$ and UV lamp on), thereby reinforcing the contribution of the immobilized photocatalyst in estradiol degradation.

During the adsorption cycles (double-stage process), the estradiol-laden MIPs were removed from solution and transferred to other flasks containing water of which some were irradiated with UV light. Figure 9 shows that in the 1st cycle of use, the adsorbents had roughly the same adsorption capacity, as expected. In the 2nd cycle, there was a small decrease in the $q_e$ values for all materials, indicating estradiol adsorption was somewhat compromised, mainly in the flasks which did not receive UV light. This trend was confirmed by the 3rd cycle of use, since a reduction in $q_e$ values was much more evident, except for MIP-$TiO_2$ submitted to the photoregeneration process with UV light. On the other hand, the MIP submitted to the same process showed a decrease in its adsorption capacity, which indicates the positive role of $TiO_2$ in enhancing the adsorbent regeneration.

Comparing the MIP with the MIP-$TiO_2$ placed in water and not submitted to photoregeneration, it can be observed that the latter exhibited a drop in its adsorption capacity that was much more expressive than the first one; this is probably related to its lower adsorption capacity, as evidenced by isotherm experiments due to the presence of the catalyst in the polymer matrix. It is believed that under optimized test conditions, photoregeneration can restore the adsorption capacity of MIP-$TiO_2$ more efficiently, prolonging its use until a saturation point is reached and, consequently, reducing the frequency of adsorbent replenishments.

By analyzing the results obtained in the photodegradation tests, it is observed that the double-stage process (Fig. 7b) is more promising since it leads to less energy expenditure. This is because the double-stage process optimizes the use of the free radicals generated by the irradiated $TiO_2$ which would be spent to degrade the target molecule and free the adsorption sites. In a combined adsorption and photodegradation system (single-stage process), part of the UV energy supplied would be spent to degrade other molecules of lower toxicity and/or higher biodegradability that might be present in a real effluent, which could contribute to less destruction of the compounds of interest, especially under lower radiation doses.

## 4 Conclusions

The results have shown that the MIP-$TiO_2$ has a good adsorption capacity for E2 and high selectivity. In addition, comparing the proposed systems for the photodegradation tests, it was noticed that the double-stage system (estradiol adsorption onto MIP-$TiO_2$ followed by the photoregeneration of the estradiol-laden adsorbent) was more promising, since it was possible to observe the maintenance of estradiol adsorption capacity of the adsorbent after 5 cycles of adsorption/regeneration of the material. This opens the possibility of using MIP-$TiO_2$ in water treatment systems to remove specific contaminants such as estradiol.

**Authors' Contributions** All authors contributed to the study conception and design. Material preparation, data collection, and analysis were performed by Marina Caldeira Tonucci and Leandro Pablo dos Santos Xavier. The first draft of the manuscript was written by Marina Caldeira Tonucci, and all authors commented on previous versions of the manuscript. All authors read and approved the final manuscript.

Conceptualization: Bruno Eduardo Lobo Baêta, Sérgio Francisco de Aquino, and Adilson Candido da Silva

Methodology: Marina Caldeira Tonucci, Leandro Pablo dos Santos Xavier

Formal analysis and investigation: Bruno Eduardo Lobo Baêta, Marina Caldeira Tonucci, Sérgio Francisco de Aquino, and Adilson Cândido da Silva

Writing, original draft preparation: Marina Caldeira Tonucci

Writing, review and editing: Marina Caldeira Tonucci, Bruno Eduardo Lobo Baêta, Sérgio Francisco de Aquino, and Adilson Candido da Silva

Funding acquisition: Bruno Eduardo Lobo Baêta and Sérgio Francisco de Aquino

Supervision: Bruno Eduardo Lobo Baêta and Sérgio Francisco de Aquino

**Funding Information** The authors are grateful to the following institutions for their financial support: the Federal University of Ouro Preto (UFOP), the Minas Gerais State Research Foundation (FAPEMIG), the Brazilian National Council for Scientific and Technological Development (CNPq), and the Coordination for the Improvement of Higher Education Personnel (CAPES).

## References

Barros, L. A., Custodio, R., & Rath, S. (2016). Design of a new molecularly imprinted polymer selective for hydrochlorothiazide based on theoretical predictions using gibbs free energy. *Journal of the Brazilian Chemical Society, 27*, 2300–2311. https://doi.org/10.5935/0103-5053.20160126.

Kalan, R. E., Yaparatne, S., Abirmahman, A., & Tripp, C. P. (2016). P25 titanium dioxide coated magnetic particles: Preparation, characterization and photocatalytic activity. *Applied catalysis B: Environmental, 185*, 249–258. https://doi.org/10.1016/j.apcatb.2016.01.008.

Kümmerer, K. (2009). The presence of pharmaceuticals in the environment due to human use – present knowledge and future challenges. *Journal of Environmental Management, 90*(8), 2354–2366. https://doi.org/10.1016/j.jenvman.2009.01.023.

Lai, C., et al. (2016). Synthesis of surface molecular imprinted TiO2/graphene photocatalyst and its highly efficient photocatalytic degradation of target pollutant under visible light irradiation. *Applied Surface Science, 390*, 368–376. https://doi.org/10.1016/j.apsusc.2016.08.119.

Lee, H.-B., Peart, T. E., & Svoboda, M. L. (2005). Determination of endocrine-disrupting phenols, acidic pharmaceuticals, and personal-care products in sewage by solid-phase extraction and gas chromatography–mass spectrometr. *Journal of Chromatography A, 1094*(1), 122–129. https://doi.org/10.1016/j.chroma.2005.07.070.

Lee, S. and Doong, R. (2012) Adsorption and selective recognition of 17ß-estradiol by molecularly imprinted polymers, *Journal of Polymer Research*, 19. https://doi.org/10.1007/s10965-012-9939-9.

Li Puma, G., et al. (2010). Photocatalytic oxidation of multicomponent mixtures of estrogens (estrone (E1), 17β-estradiol (E2), 17α-ethynylestradiol (EE2) and estriol (E3)) under UVA and UVC radiation: Photon absorption, quantum yields and rate constants independent of photon absorption. *Applied Catalysis B: Environmental, 99*(3), 388–397. https://doi.org/10.1016/j.apcatb.2010.05.015.

Li, Y., et al. (2006). Synthesis of Magnetic Molecularly Imprinted Polymer Nanowires Using a Nanoporous Alumina Template. *Macromolecules, 39*(13), 497–4499. https://doi.org/10.1021/ma0526185.

Nawi, M. A., & Zain, S. M. (2012). Enhancing the surface properties of the immobilized Degussa P-25 $TiO_2$ for the efficient photocatalytic removal of methylene blue from aqueous solution. *Applied Surface Science, 258*(16), 6148–6157.

Oi, L. E., et al. (2016). Recent advances of titanium dioxide (TiO2) for green organic synthesis. *RSC Advances, 6*(110), 108741–108754. https://doi.org/10.1039/C6RA22894A.

Oliveira, L. C. A., Silva, A. C., & Pereira, M. C. (2015). Peroxoniobium oxyhydroxide sensitized TiO2 crystals. *RSC Advances, 5*(55), 44567–44570. https://doi.org/10.1039/C5RA07343J.

Paz, Y. (2010). Application of TiO2 photocatalysis for air treatment: Patents' overview. *Applied Catalysis B: Environmental, 99*(3), 448–460. https://doi.org/10.1016/j.apcatb.2010.05.011.

Saavedra, L. N. M., et al. (2017). Thermodinamic study of a magnetic molecular imprinted polymer for removal of nitrogenous pollutant from gasoline. *Fuel, 210*, 380–389. https://doi.org/10.1016/j.fuel.2017.08.087.

Saavedra, L. N. M., et al. (2018). Molecularly imprinted polymers for selective adsorption of quinoline: theoretical and experimental studies. *RSC Advances, 8*(50), 28775–28786. https://doi.org/10.1039/C8RA04261F.

Shayegan, Z., et al. (2018). Effect of surface fluorination of P25-$TiO_2$ on adsorption of indoor environment volatile organic compounds. *Chemical Engineering Journal, 346*, 578–589.

Shen, X., et al. (2012). Molecular imprinting for removing highly toxic organic pollutants. *Chemical Communications, 48*(6), 788–798. https://doi.org/10.1039/C2CC14654A.

Xavier, L. P. d. S., et al. (2019). Experimental and theoretical studies of solvent polarity influence on the preparation of molecularly imprinted polymers for the removal of estradiol from water. *New Journal of Chemistry, 43*(4), 1775–1784. https://doi.org/10.1039/C8NJ03639J.

Xu, S., et al. (2014). Molecularly imprinted TiO2 hybridized magnetic Fe3O4 nanoparticles for selective photocatalytic degradation and removal of estrone. *RSC Advances, 4*(85), 45266–45274. https://doi.org/10.1039/C4RA06632D.

Zhang, J., Wang, L., & Han, Y. (2013). Preparation of 17β-estradiol surface molecularly imprinted polymers and their application to the analysis of biological samples. *Journal of Separation Science, 36*(21–22), 3486–3492. https://doi.org/10.1002/jssc.201300850.

Zhao, Y., et al. (2015). Preparation of molecularly imprinted polymers based on magnetic carbon nanotubes for determination of sulfamethoxazole in food samples. *RSC Advance, 5*(86), 70309–70318. https://doi.org/10.1039/C5RA13183A.